energies

MDPI

Article

Enhancement in Efficiency of CIGS Solar Cell by Using a p-Si BSF Layer

Meriem Chadel [1,*], Asma Chadel [1], Boumediene Benyoucef [1] and Michel Aillerie [2]

[1] Unité de Recherche Matériaux et Énergies Renouvelables, URMER, University of Tlemcen, BP 119, Tlemcen 13000, Algeria
[2] Laboratoire Matériaux Optiques, Photonique et Systèmes (LMOPS), Université de Lorraine, CentraleSupélec, F-57000 Metz, France
* Correspondence: ch.meriem.ph@gmail.com; Tel.: +213-667294959

Abstract: Copper–indium–gallium–diselenide Cu(In,Ga)Se_2 (CIGS) is a semiconductor compound belonging to group I-III-VI, with a chalcopyrite crystal structure. CIGS is promising for the development of high-performance photovoltaic applications in terms of stability and conversion efficiency. It is one of the main candidates to rival the efficiency and stability of conventional crystalline silicon cells, due to its high light absorption coefficient, lower material cost, and high stability. The limitation of its use is that CIGS integrates indium (In) and gallium (Ga), which are rare and expensive materials. The amount of these materials in the CIGS cell can be reduced by optimizing the thickness of the absorber. We show that the introduction of a layer of highly doped silicon in the structure of the solar cell between the absorber layer and the back surface field layer effectively allows for decreasing the thickness of the absorber. Within the same objective, we focus on the danger of cadmium in the CdS buffer layer. In the first optimizations, we replaced the n-type CdS buffer layer with a n-type Zn(O,S) buffer layer. For this work, we used a one-dimensional simulation program, named Solar Cell Capacitance Simulator in one Dimension (SCAPS-1D), to investigate this new CIGS solar cell structure. After optimization, a maximum conversion efficiency of 24.43% was achieved with a 0.2 µm CIGS absorber layer and a 1 µm Si BSF layer.

Keywords: ultra-thin CIGS; Si BSF layer; graded absorber layer; Zn(O,S) buffer layer

check for updates

Citation: Chadel, M.; Chadel, A.; Benyoucef, B.; Aillerie, M. Enhancement in Efficiency of CIGS Solar Cell by Using a p-Si BSF Layer. *Energies* **2023**, *16*, 2956. https://doi.org/10.3390/en16072956

Academic Editor: Vesselin Donchev

Received: 8 February 2023
Revised: 22 February 2023
Accepted: 3 March 2023
Published: 23 March 2023

Copyright: © 2023 by the authors. Licensee MDPI, Basel, Switzerland. This article is an open access article distributed under the terms and conditions of the Creative Commons Attribution (CC BY) license (https://creativecommons.org/licenses/by/4.0/).

1. Introduction

In the last decade, the efficiency of Cu(In,Ga)Se2 (CIGS) based solar cells improved from 20% [1,2] to 22.6% [3]. This growth in efficiency was achieved by the integration of the solar cell structure with a CIGS absorber layer with a high optical absorption coefficient [3]. The development of thin film solar cell technology, associated with recent progress in the manufacturing process, allows for an increase in the commercial demand of CIGS cells for specific markets. The advantage of CIGS cells is the long-term stability of this structure, which will decrease the final cost over time while improving its competitiveness [2,4]. Nevertheless, indium (In) and gallium (Ga) are rare and expensive materials, and the long-term development of this technology is linked to the reduction of the usage of these two elements in the absorber layer. Reducing materials usage is important for indium (In) and gallium (Ga) since the supply of these metals may become a problem if CIGS thin film solar cells are produced in large quantities [5,6]. A possible way to accomplish that is to take the opportunity offered by the Cu(In,Ga)Se2 compound to change its In/Ga ratio, resulting in a change of its band gap from 1.02 eV to 1.68 eV [7,8] according to the percentage of gallium (Ga) content in CIGS layer [9]. This ratio can be constant or graded in the CIGS absorber layer. Nevertheless, as experimentally shown by Rau et al. [10] and Hanna et al. [11], the increase in the band gap by introducing gallium creates defects in the volume of the absorber. These defects become detrimental to device performance when the gap exceeds 1.15 eV. Thus, considering In and Ga concentrations as given and fixed

parameters due to the solar spectral range and the technological constraints, the second possibility that can be used for the improvement of the efficiency of the cell and to the decrease usage of the elements is by modifying the thickness of the absorber layer. Thus, optimization of CIGS cells with thinner CIGS absorbers is a way to increase the throughput of a factory and reduce material consumption.

Nowadays, the CIGS absorber layer has a typical thickness of about 1–2 µm [12,13]. However, on the way towards mass production, and for the above-mentioned reasons, it will be necessary to reduce the thickness even further by the optimization of the simulation process of a cell based on the following structure: graded $Cu(In_{1-x},Ga_x)Se_2$/CdS/ZnO and Al:ZnO as a superficial transparent conductive oxide (TCO) layer. H. Movla in [14] found that a high efficiency (20.34%) can be achieved when using the graded CIGS absorber layer with a thicknesses of 0.5 µm and a TCO layer equal to 20 nm. However, on the experimental side, B. Vermang et al. [15], by employing Si solar cell technology, has increased the efficiency of ultra-thin Cu(In,Ga)Se2 solar cells up to, but currently limited to, 13.5% using a CIGS absorber layer with a thickness of 0.385 µm. Otherwise, it was shown that [16,17] the integration of a very thin absorber layer will affect the cell performance, as the carrier lifetime is reduced and the carrier recombination increases in the back surface layer. Moreover, some portions of the incident photons will be lost in the region of the back contact materials, which will further reduce the generation rate of electronic carriers, but only a few studies have been led on the possible solutions to the problems arising from the use of an ultra-thin CIGS absorber. Considering this issue, the first approach to improve the performance of ultra-thin CIGS cells is the grading in the composition of the absorber layer, inducing a graded band gap [13,16]. Different types of grading profiles were developed, such as linear or exponential. With this grade in the band-gap, we can achieve a quasi-Back Surface Field BSF which creates an electric field in the back surface region to reflect the minority carrier electrons and force them towards the front contact region [18]. A second approach is an implementation of the structure of an additional highly doped layer, a BSF layer between the absorber and the back contact layers [16,17]. Different types of BSF for CIGS solar cells were developed, such as those based on Tin Selenide (SnSe) [17] or Tin Sulfide (SnS) [19]. It is to be noted that this last material is used as a BSF in Cu(Zn,Sn)S (CZTS) solar cells [20].

In the present work, an alternative structure of CIGS solar cells based on ZnO/CdS/CIGS/Si thin layers is suggested, numerically analyzed, and optimized using the one-dimensional SCAPS-1D simulator, developed by Gent University [21,22]. We especially focus on the optimization of the absorber layer thickness and the influence of the BSF on the electrical parameters of CIGS solar cells. An investigation into the effects of band gap grading on the performance of ultra-thin CIGS solar cells is also carried out. Finally, with the aim of sustainability, we replace the buffer layer CdS, because it is highly toxic [23] due to cadmium, with a non-toxic oxysulfide of zinc(Zn(O,S))layer and continue the optimization process.

2. Solar Cell Structure

Figure 1a presents the structure of the reference CIGS solar cell developed by Jackson et al. [24], which will serve as a starting reference in the current study. In this structure, a CIGS absorber layer is deposited by co-evaporation, with a thickness ranging from 2.5 to 3 µm, on a molybdenum (500–900 nm)/glass substrate. This absorber layer is covered by an N-type CdS (30–50 nm) layer deposited by CBD, which ensures the formation of the heterojunction. An intrinsic ZnO (50–100 nm) buffer layer and Al-doped ZnO (150–200 nm) transparent conductive window constitute the superficial layers. Finally, metal flat bands enable the Ohmic electrical contacts.

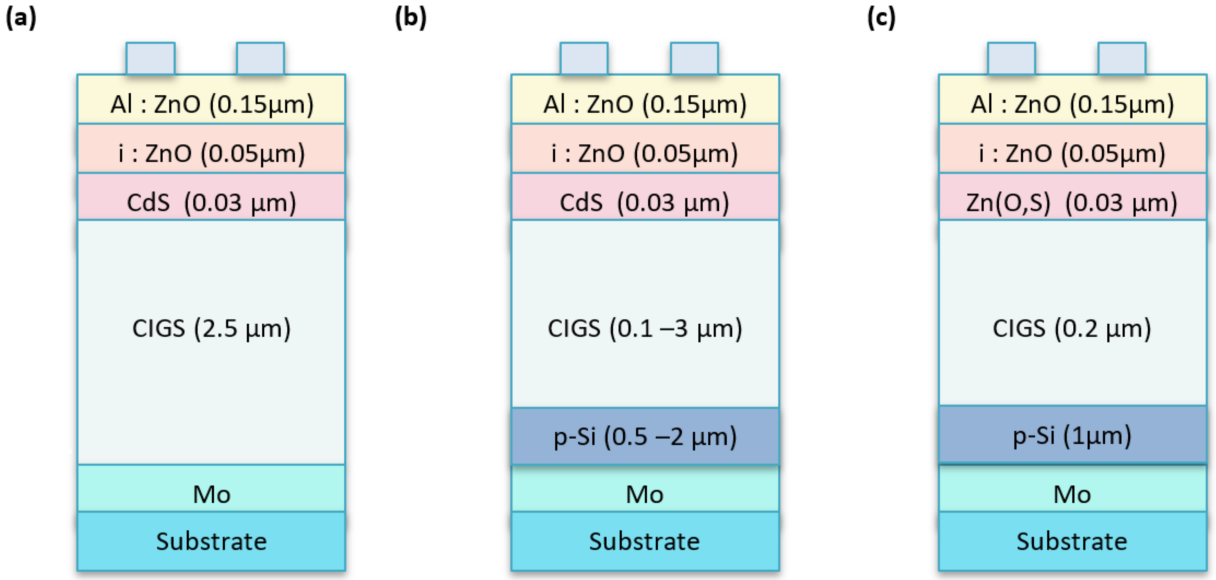

Figure 1. Schematic view of: (**a**) CIGS solar cells. (**b**) New ultra-thin CIGS structure with BSF. (**c**) New ultra-thin CIGS structure with BSF and Zn(O,S) buffer layer.

The band gap of CIGS ranges from 1.02 eV to 1.68 eV with the Ga/In mole fraction. This change occurs primarily in the conduction band through the substitution of Ga atoms for In atoms [25]. With x = Ga/(Ga + In), the band gap energy can be calculated as follows [26]:

$$E_g = 1.02 + 0.39238x + 0.24762x^2 \quad (1)$$

With a band gap of approximately 1.15 eV and a Ga content of approximately 30% [10,11], CIGS solar cells experimentally achieve a conversion efficiency of approximately 20%. In the reference structure [24,27], the authors have chosen the ratio where Cu/(Ga + In) = 0.91 and the ratio where x = Ga/(Ga + In) = 0.32, yielding a band gap equal to 1.13 eV. The optical absorption constant can be set from either from a model or from a file in the software SCAPS [21,22]. The coefficient of CIGS at different x ratios is taken from the Gloeckler model [28], and we can calculated the absorption coefficient using the following equation [29]:

$$a = A(h\,v - E_g)^{1/2} \quad (2)$$

where A is the constant of proportionality, which depends on the densities of the states related to the photon absorption and the irradiation energy. E_g is the band-gap of the material, and $h\,v$ is the photon energy of the incident radiation. The model of the optical absorption used in the SCAPS for the CIGS solar cell is based on the experimental results presented in Alonso et al. [8].

As shown in Figure 1b, in the new structure, we have, added from the reference, a p-Si layer with a gap equal to 1.12 eV. The role of this new absorber layer on photovoltaic cell parameters was examined using the SCAPS computer software program for various thicknesses of CIGS absorber layer, from 0.1 to 3.0 µm. The Si and CIGS p-type absorber layer has a thickness of 1 µm, deposited on molybdenum-connected back-glass substrate.

Currently, cadmium sulfide (CdS) is used as a buffer layer in most of the CIGS-based solar cells [30]. However, cadmium is toxic and harmful to the environment [12,30]. Furthermore, the bandgap of CdS is about 2.4 eV [31], which is not large enough to transmit all the parts of visible light and limits the further enhancement of light-to-electricity conversion efficiency. A. Chadel et al., in ref. [32], showed that the solar cell based on CIGS/Zn(O_{1-x},S_x) attains an electrical performance equivalent to the solar cell based on CIGS/CdS. Oxysulfide of zinc (Zn(O,S)) is not toxic, it has a band gap energy (E_g) ranging from 2.7 eV to 3.6 eV [33], and it is deposited on the CIGS with the co-sputtering PVD,

which is less expensive than chemical bath deposition. Thus, it is interesting to envisage the replacement of CdS in the buffer layer by Zn(O,S). This new structure with a Zn(O,S) buffer layer as shown in Figure 1c.

The parameters that need to be defined are thickness, electron–hole mobility, intrinsic carrier concentration, electron affinity, band gap and doping density for absorber, buffer, and window layers. The properties of the materials used in this simulation were based on experimental data, literature values [17,28,34–36], and, in some cases, reasonable estimation. The basic values were optimized and the properties of the material used are presented in Table 1. The specific values of the Rs (series resistance) and Rp (parallel resistance) given in the reference are as follows: Rs = 0.32 Ω cm^2, Rp = 1.76 kΩ cm^2 [24]. The silicon parameters given in the table are extracted from [37].

Table 1. Baseline parameters for modeling CIGS solar cells.

Layer Properties						
	Al:ZnO [17,37]	i:ZnO [28,34–36]	CdS [17,28,34–37]	CIGS [17,28,34–37]	p- Si [28,35–37]	Zn (O,S) [17,35,36]
Thickness (μm)	0.15	0.1	0.03	0.1–3	0.5–2	0.03
Dielectric permittivity	9	9	10	13.6	11.9	9
Electron mobility (cm^2/V.s)	100	100	100	100	1450	100
Hole mobility (cm^2/V.s)	25	25	25	25	500	25
Energy of gap (eV)	3.3	3.3	2.4	1.13	1.12	2.9
Effective CB density of states (cm^{-3})	2.2×10^{18}	2.2×10^{18}	2.2×10^{18}	2.2×10^{18}	2.8×10^{19}	2.2×10^{18}
Effective VB density of states (cm^{-3})	1.8×10^{19}	1.8×10^{19}	1.8×10^{19}	1.8×10^{19}	2.65×10^{19}	1.8×10^{19}
Electron thermal velocity (cm s^{-1})	10^7	10^7	10^7	10^7	10^7	10^7
Hole thermal velocity (cm s^{-1})	10^7	10^7	10^7	10^7	10^7	10^7
Electron affnity (eV)	4	4.45	4.2	4.5	4.05	4
Shallow donor density ND (cm^{-3})	10^{18}	0	10^{18}	–	–	10^{18}
Shallow acceptor density NA (cm^{-3})	–	0	–	2×10^{16}	10^{20}	–
Bulk defect properties						
Capture cross-section elect (cm^2)	10^{-12}	10^{-12}	10^{-13}	5×10^{-13}	5×10^{-13}	10^{-12}
Capture cross-section hole (cm^2)	10^{-12}	10^{-12}	10^{-13}	1×10^{-15}	5.07×10^{-15}	10^{-12}

3. Results and Discussion

3.1. Energy Band Diagram

The band diagrams for the structures of CIGS/CdS/i:ZnO/Al:ZnO and Si/CIGS/CdS/i:ZnO/Al:ZnO solar cells are represented in Figures 2 and 3, respectively. We simulated these energy bands using SCAPS. Energy band diagrams help in explaining the properties of both photovoltaic cells. We observed that there was a good band alignment between the Si and the CIGS absorber layers. It should be noted that the defect is taken into account in each layer, as well as in the interface between $Cu(In_{0.7},Ga_{0.3})Se_2$ and Si.

The electron affinity and the values of the band gap of the semiconductors are considered to calculate ΔE_C and ΔE_V. Thus, we can readily identify the band bending that occurs between in the Si/CIGS junction. We also observed a "spike" formed with ΔE_C~+0.3 eV at the CIGS/CdS junction.

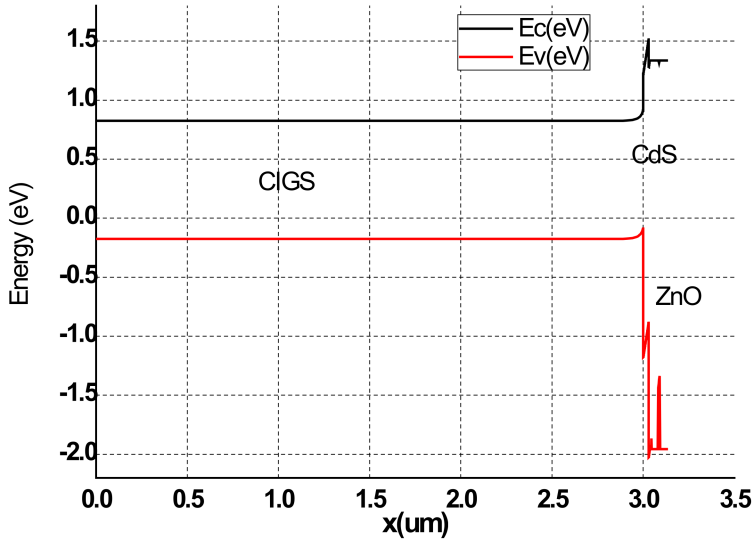

Figure 2. Band diagram for CIGS structure solar cells without BSF.

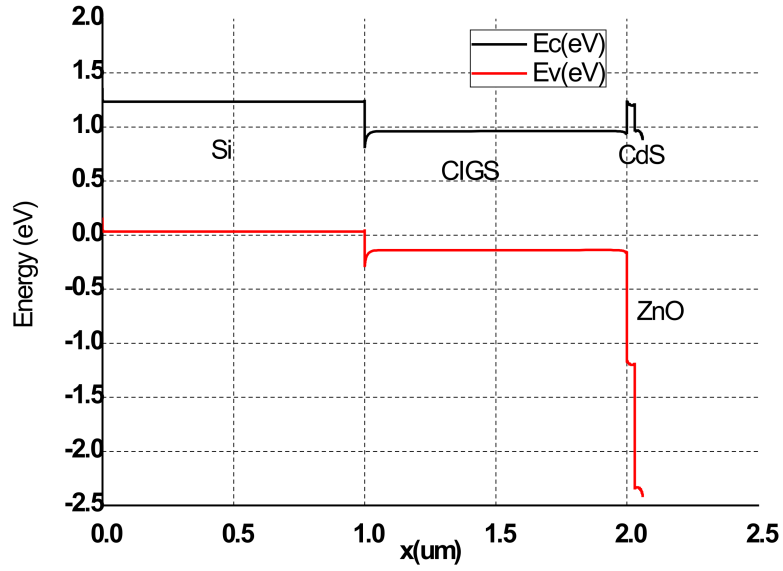

Figure 3. Band diagram for CIGS structure solar cells with BSF.

3.2. J–V Characteristics

Figure 4 shows a superposition of the J–V curve of the reference CIGS solar cell and both proposed structures, CIGS/CdS/i:ZnO/Al:ZnO and Si/CIGS/CdS/i:ZnO/Al:ZnO, presented in Figure 1, where the absorber thickness is taken as the default thickness of 3µm. The resulting performance parameters of the open-circuit voltage, short-circuit current density, fill factor, and efficiency are shown in Table 2. The efficiency of the reference cell was found to be equal to 20.8%; this value is compared with the efficiency value found by the simulation of 19.24%. Although the experimental values are more advanced than the simulated ones, excellent agreement was observed in the J–V characteristic. The accordance between the experiment and the simulation for the J–V characteristic validates our set of parameters as a baseline for simulating the influence of the variation of absorber parameters on the solar cell's performance.

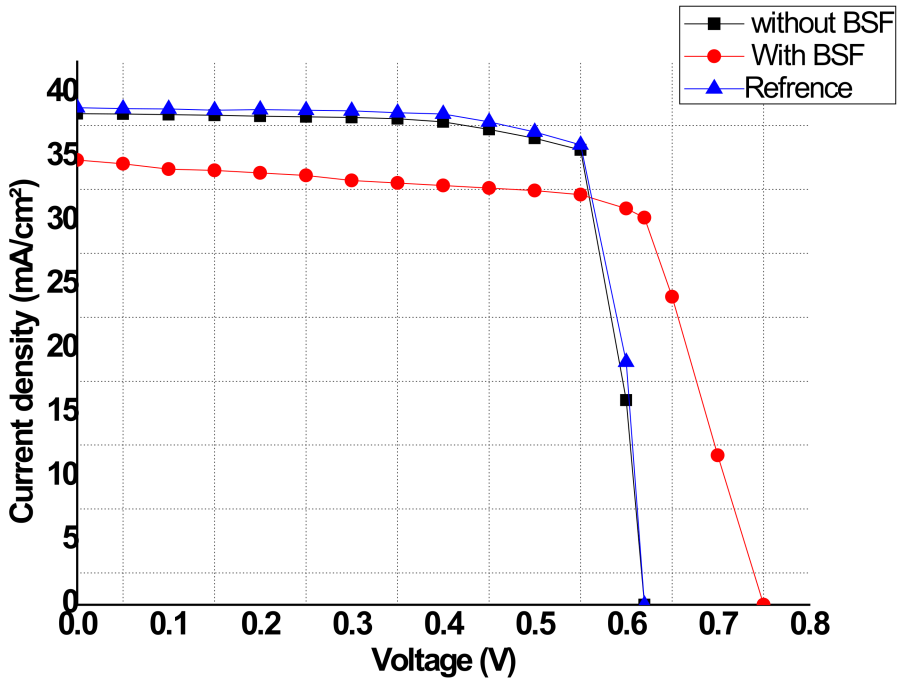

Figure 4. J–V Characteristics of the different structure of the CIGS solar cell.

Table 2. Results from simulation compared with experimental data and with solar cell with a BSF layer.

	V_{OC}	J_{SC}	FF	η
Reference	0.75	34.8	79.1	20.8
Simulation	0.64	38.42	77.14	19.24
With BSF	0.65	38.89	76.34	19.49

By joining 1 µm of the new layer, Si of p-type, the efficiency was increased from 19.24%, for the reference CIGS structure, to 19.49% for the new structure. Moreover, as shown in Figure 4, the cell efficiency increases when the absorbing layer is thicker. Our results showed that, for a CIGS thickness of 3 µm, an efficiency of 19.49% was achieved. This is mainly owing to the thickness of the absorber layer, such that more photons can be absorbed and more electron–hole pairs are generated. This slightly increases J_{SC} and V_{OC}, and thus the efficiency is improved. To explain the observed results, we recall that the BSF layer keeps the minority carriers in the CIGS absorbing layer far from the high recombination with the carriers of the back contact. Thus, for the back surface fields, the conduction band is at its highest level, and the valence band is at its lowest possible level. The performances of both solar cells, with and without Si, are summarized in Table 2.

3.3. Effect of CIGS Absorber Layers Thickness

The performance parameters of the cell, J_{SC}, V_{OC}, FF, and efficiency (η) of the CIGS solar cell as a function of the thickness of the absorber layer for both solar cells, with and without Si (BSF), are shown in Figure 5. The thickness of CIGS changes from 0.1 µm to 3 µm, while other input parameters are kept unchanged. Figure 5, without BSF layer, presents the effects on cell performance parameters with different thicknesses of the CIGS absorber layer. It is well understood that with an increase in the thickness of CIGS absorber layers, all parameters increase up to 2 µm; after 2 µm, they increase only slightly. The J_{SC} passes from 26.5 to 38.42 mA/cm^2. This is primarily due to the recombination of photo-generated electrons at the back contact (Mo) [38,39]. We remark that the VOC passes from 0.46 to 0.64 V. A thin absorber layer means that the back contact and the depletion regions are

very physically close to each other, which enhances the capturing of electrons by the back contact. This form of recombination process is prejudicial to cell performance as it affects both V_{OC} and J_{SC}. The thickness of absorber layer increases the efficiency increases from 7.67% to 19.24%. The increase in the conversion efficiency is mainly due to the increase in the p-type $CuIn_{0.7}Ga_{0.3}Se_2$ absorber layer. As the p-type layer grows, most photons in long wavelengths can be collected in the absorber layer [16,31].

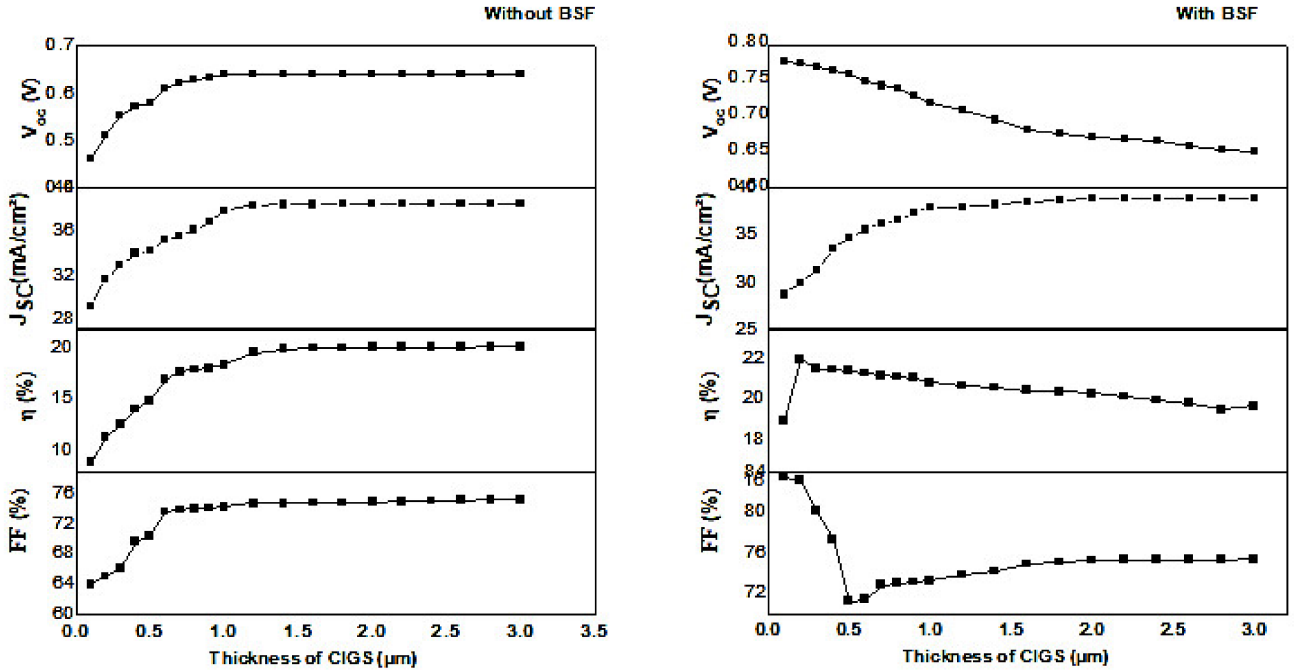

Figure 5. The performance of the solar cell without and with BSF as a function of CIGS thickness.

The recombination of electrons at the back contact is due to the depletion region being very close to the back contact. Furthermore, the CIGS/Mo interface has a high recombination velocity [40] which improves the electron-catching process during cell operation. To increase the efficiency of the ultra-thin CIGS solar cells, the carrier recombination at the back surface must be reduced. One of the practical ways is to introduce a back surface field (BSF). Moreover, this layer decreases the back contact barrier height and reduces minority carrier recombination loss [41,42]. The influence of the thickness of the CIGS absorber layer on the performance of the proposed cell with BSF is shown in Figure 5. By incorporating the BSF layer, when the absorber layer increases from 0.1 to 3 μm, the J_{SC} increases from 28.65 to 38.89 mA/cm^2, and V_{OC} decreases slightly from 0.776 V to 0.65 V. The Si BSF layer reduces carrier recombination losses and improves carrier movement due to migration. This phenomenon leads to an increase in the short-circuit current and a drop in the open-circuit voltage. The decrease in the open-circuit voltage is explained by the existence of the leakage current or diode current. Thus, it can be seen that the open-circuit voltage follows the same variation as the fill factor. This effect was also previously confirmed by the relationship between FF and V_{OC} as shown in the examples defined in Todorov et al. [43] and Green [44]. Finally, the cell efficiency increases rapidly when the Si layer is fused to act as a BSF layer (10^{20} cm^{-3} doping) adjacent to the CIGS absorber layer (2×10^{16} cm^{-3} doping). The interface between p+-type Si and p-type CIGS acts as a p–n junction. The electric field thus created acts as a barrier to the flow of minority carriers towards the rear surface. The simulation results show that a 0.2 μm thick CIGS layer can be considered as optimal, a value which will be applied in the rest of the study. This result is confirmed by Duchatelet et al. [45], who showed that an absorber layer thickness of 0.3 to 0.7 μm is sufficient to absorb almost all of the incident solar radiation due to the direct band gap and

the materials related to chalcopyrite. This small discard of 0.1 is the difference between the simulations and the experiment, and it confirms that we are not far from the theory.

It is known that indium and gallium are rare, dangerous, and expensive materials, and, therefore, the production of thin absorbers in CIGS-based solar cells is recommended. Furthermore, silicon is more available, less harmful, and less expensive than indium and gallium. Our study shows that its integration in the CIGS solar cell structure has a certain interest because the efficiency of new cells resulting from its integration is high, and the costs are reduced.

3.4. Effect of Si Back Surface Field Layer Thickness

Figure 6 shows the performance of the solar cell with BSF according to the thickness of the BSF Layer (Si). The thickness of the BSF layer was changed from 0.5 µm to 2 µm while all the remaining parameters of the solar cell were kept constant. Simulated fallouts show that, with an increase in the thickness of the BSF layer, a very small variation is observed in the functional parameters, i.e., in J_{SC}, V_{OC}, η, and FF, such as the efficiency η, which decreases from 21.53% to 21.45%. This result shows that an increase in BSF layer thickness does not affect the output of the proposed device. In the design of Si/CIGS solar cells, the optimum thickness of the BSF layer is 1 µm.

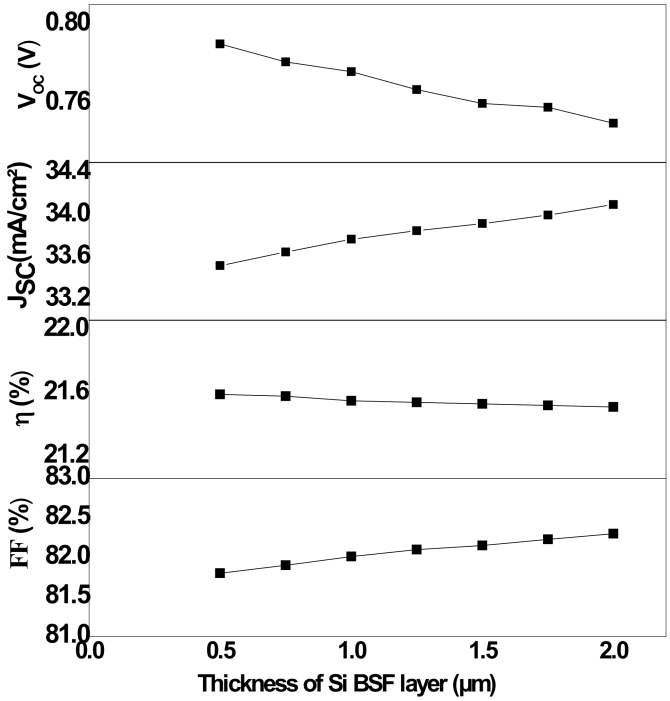

Figure 6. The performance of the solar cell with BSF as a function of Si BSF layer thickness.

3.5. Effect of Ga-Grading on the Cell Performance

Several research groups have studied the effect of varying the band gap on the performance parameters of the solar cell based on CIGS [10,11,25,40]. $Cu(In_{1-x}Ga_x)Se$ has a variable band gap of 1.02 eV ($CuInSe_2$) to 1.68 eV ($CuGaSe_2$). The variation of the absorber layer band gap is consistent with the variation of its electron affinity and is related to changes in its optical absorption [7,26]. The optical absorption coefficient of CIGS at different Ga/(Ga + In) ratios (GGI ratio) is given from the Gloeckler model [28]. With an exponential band gap profile, the electron affinity is quasi-independent of the composition; this situation is called 'E_C grading' [46]. With an exponential band gap profile and 0.2 µm thickness of graded-CIGS, we analyze the J–V characteristic shown in Figure 7. The other parameters of the absorber, as well as the properties of the other layers of the cells, are assumed to be steady in this work, such as the thickness of BSF at 1 µm. Table 3 compares the

performance parameters of the new structure with a graded-CIGS and with an ungraded CIGS with the same thickness as the CIGS and BSF.

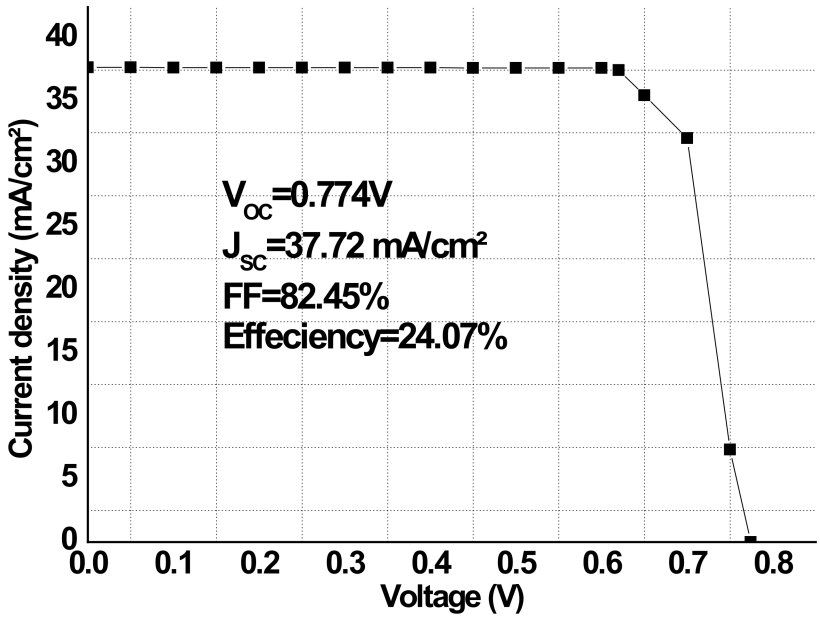

Figure 7. J–V characteristics curve of the solar cell based on graded CIGS.

Table 3. Results of the performance parameters for graded CIGS compared with data of the ungraded CIGS.

	V_{OC}	J_{SC}	FF	η
Ungraded-CIGS	0.777	33.73	81.99	21.51
graded-CIGS	0.774	37.72	82.45	24.07

We can see in Table 3 that the JSC and η of both structures are largely different, such as the J_{SC} increase from 33.73 to 37.72 mA/cm^2 and the η increase from 21.51% to 24.07%. For an absorber thickness of 0.2 µm, the gain in efficiency is around Δη = 2.51%. It is the same result obtained by O. Lundberg et al. in [40] for a thickness of 0.5 µm. These developments in J_{SC} are due to the passivation of the back contact, which is increasingly prejudicial to the device performance when the CIGS thickness is reduced. Moreover, for pure CIS, a significant improvement in the device performance is obtained by introducing an increased Ga concentration towards the back contact. This improvement is, however, more related to the introduction of Ga itself than to the gradient of the Ga-concentration. From many simulations, the largest gain is predicted for an increased Ga/(In + Ga) ratio towards the CIGS surface [40].

3.6. Insert Buffer Layer without Cadmium

The CdS layer, as shown in Figure 1, acts as a buffer layer between the highly conductive window layer, ZnO, and the absorber layer, $CuIn_{1-x}Ga_xSe_2$. It contains the highest level of carcinogenic cadmium. Therefore, several research groups have studied replacing this material with another that is not toxic, such as In_2S_3 [47], ZnS [30], ZnSe [48], $Zn_{1-x}Mg_xO$ [49], and Zn(O,S) [32,50]. We chose Zn(O,S) because of its excellent optical and electrical properties, which are related to its high band gap that ranges from 2.7 eV to 3.6 eV [33]. The exact value of the E_g depends on x, namely, the (S/S + O) ratio. It is non-toxic, and it is deposited on the CIGS with co-sputtering PVD [33]. A. Okamoto et al. [51] found that the CIGS solar cell with the $Zn(O_{0.82}S_{0.18})$ (S/S + O) = 0.18 corresponding to E_g = 2.9 eV) buffer layer showed a higher J_{SC} than that with the CdS buffer layer, and the

efficiency of the CIGS solar cell with the proposed buffer layer approached that of the CIGS solar cell with the CdS buffer layer. All parameters of Zn(O,S) are listed in Table 1.

The current–voltage (J–V) characteristics of the new structure Zn(O,S)/graded-CIGS/Si with a Zn(O,S) buffer layer, are shown in Figure 8 and are within 0.2 µm and 1 µm of graded-CIGS and Si, respectively. The performance parameters of both structures, CdS/graded-CIGS and $Zn(O_{0.82}S_{0.18})$/graded-CIGS, are illustrated in Table 4. We note that the J_{SC} and efficiency are slightly increased, from 37.72 to 38 mA/cm^2 and 24.07% to 24.43%. This is due to a decrease in the absorption loss in the Zn(O,S) buffer layer, which has a wider energy band gap than CdS ($E_{gZn(O,S)} > E_{gCdS}$). These results are very much in agreement with the results found by references [32,51,52].

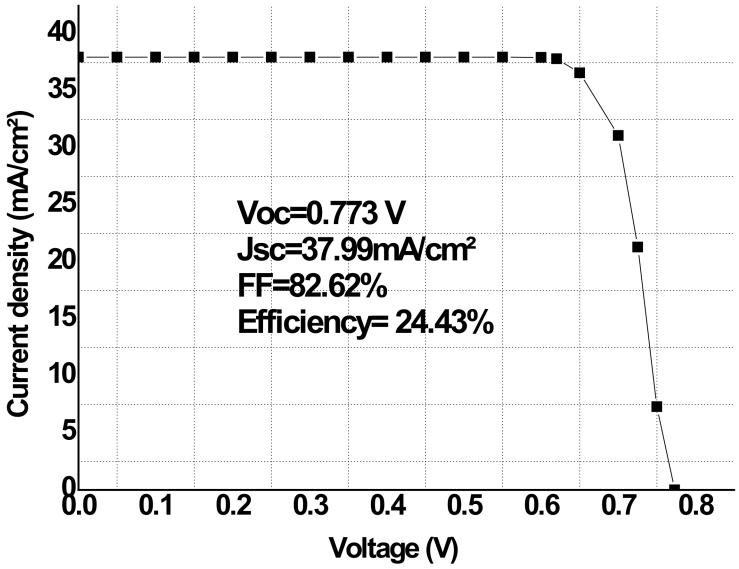

Figure 8. J–V characteristics of the new structure Zn(O,S)/graded-CIGS/Si.

Table 4. Performance parameters of the both structures: CdS/graded-CIGS and $Zn(O_{0.82}S_{0.18})$/graded-CIGS.

	V_{OC}	J_{SC}	FF	η
Zn(O,S)/CIGS	0.773	38	82.62	24.43
CdS/CIGS	0.774	37.72	82.45	24.07

Finally, considering the cell structure and its various layers, we discuss the pertinence of the results obtained by modeling the performance of a CIGS cell, as performed in the current work, compared to the performance of commercial cells. Recent theoretical research [53,54] proves the advantageous effect of a p-silicon layer on the performance of CIGS solar cells. The results propose a silicon layer associated to the absorber layer and point out the fact that more photo-generated carriers improve the cell performance. In addition, this layer can have good contact with molybdenum [55]. This could make back contact of solar cell more Ohmic by decreasing the carrier recombination in the back contact layer. In [56], S. Djoumi et al. fabricated a nano/micro hybrid structure solar cell. The emitter and back surface field (BSF) layers were formed by the spin-on-dopant method. In ref. [57], Ramanujam et al. detailed the fabrication of CIGS based solar cells with and without a BSF layer. The CIGS films were prepared by a three-stage co-evaporation technique, allowing a double-graded conduction band profile with a deep notch point closer to the absorber's front surface.

It should also be noted that low-cost production of high-efficiency and long-term stable cells are critical factors for the large-scale commercialization of CIGS solar cells. The stability of CIGS solar cells is discussed in ref. [57], showing the advantage of adding a

BSF layer to the structure. In the CIGS solar cell, a graded bandgap can be achieved by fine-tuning the (Ga)/(Ga + In) ratio, and Cu can be used advantageously to synthesize CuInSe2 from the Cu substrate. Furthermore, in thin-film solar cells, there are some specific concerns: (a) the lack of flexible substrates that meet minimum requirements, (b) the use of a high-temperature process, (c) the integration of metals and polymers, and, (d) most of these metals contain a large amount of impurities. Among the metals used, Cu and Al can withstand high temperature treatment. Nevertheless, they have a high density of impurities, a high coefficient of thermal expansion, and a high roughness. Contamination due to the diffusion of undesirable elements from the metal sheets to the absorbers is disadvantageous for the global performance of the cell.

4. Conclusions

To obtain a thin solar cell with high efficiency, we added 1 µm of silicon (Si) as the back surface field (BSF) layer on a solar cell based on CIGS. We analyzed and simulated, on SCAPS simulator software, the thickness of the absorber layer (CIGS) when this layer is ungraded and exponentially graded. The simulation results show that the efficiency is 21.51% for ungraded CIGS and 24.07% for graded CIGS for the same thickness of the absorber layer. Finally, we replaced the toxic buffer layer, CdS, with oxysulfide of zinc (Zn(O,S)).

The values obtained from the proposed solar cell were: power conversion efficiency of 24.43% and fill factor (FF) of 82.62%, short circuit current (J_{SC}) of 38 mA/cm^2. and open circuit voltage (V_{OC}) of 0.773 V. These results found that the best structure must have a window layer (Al-doped ZnO) with thicknesses of 0.15 µm and 0.05 µm for intrinsic ZnO, a buffer layer (Zn(O,S)) with a thickness of 0.03 µm, an absorbent layer with a thickness of 0.2 µm, and Si with a thickness of 1 µm. The results showed that the new ultra-thin CIGS solar cells structure without Cd has a performance that is comparable to that of the conventional solar cell, with a decreased price.

Author Contributions: M.C., A.C., B.B. and M.A. conceived and planned the experiments. M.C. carried out simulations. All authors provided critical feedback and helped shape the research, analysis. M.C. took the lead in writing the manuscript and M.C. and M.A. contributed to the final version. All authors have read and agreed to the published version of the manuscript.

Funding: This research received no external funding and the APC was funded directly by the authors themselves from their own research budget as required by their institutions on which they depend.

Data Availability Statement: Data sharing does not apply to this article as it is a new modeling analysis based on literature data, all referenced in the publication. The data presented in this study as analysis results are original and presented in a coherent way because all the results are detailed and analyzed.

Acknowledgments: The authors acknowledge the use of SCAPS-1D program developed by Marc Burgelman and colleagues at the University of Gent in all the simulations reported in this paper. Authors would like to thank Maroua Houria Guitouni tor proofreading the article.

Conflicts of Interest: The authors declare no conflict of interest.

References

1. Jackson, P.; Hariskos, D.; Lotter, E.; Paetel, S.; Wuerz, R.; Menner, R.; Wischmann, W.; Powalla, M. New world record efficiency for Cu (In, Ga) Se_2 thin-film solar cells beyond 20%. *Prog. Photovolt. Res. Appl.* **2011**, *19*, 894–897. [CrossRef]
2. Reinhard, P.; Chirilă, A.; Blösch, P.; Pianezzi, F.; Nishiwaki, S.; Buechelers, S.; Tiwari, A.N. Review of progress toward 20% efficiency flexible CIGS solar cells and manufacturing issues of solar modules. In Proceedings of the 2012 IEEE 38th Photovoltaic Specialists Conference (PVSC) PART 2, Austin, TX, USA, 3–8 June 2012; pp. 1–9.
3. Jackson, P.; Wuerz, R.; Hariskos, D.; Lotter, E.; Witte, W.; Powalla, M. Effects of heavy alkali elements in Cu (In, Ga) Se_2 solar cells with efficiencies up to 22.6%. *Phys. Status Solidi RRL Rapid Res. Lett.* **2016**, *10*, 583–586. [CrossRef]
4. Gorji, N.E.; Reggiani, U.; Sandrolini, L. Surface photovoltage spectroscopy and AFM analysis of CIGSe thin film solar cells. *Int. J. Photoenergy* **2015**, *2015*, 829530. [CrossRef]

5. Lundberg, O.; Bodegård, M.; Malmström, J.; Stolt, L. Influence of the Cu (In, Ga) Se_2 thickness and Ga grading on solar cell performance. *Prog. Photovolt. Res. Appl.* **2003**, *11*, 77–88. [CrossRef]
6. Kaelin, M.; Rudmann, D.; Tiwari, A.N. Low cost processing of CIGS thin film solar cells. *Sol. Energy* **2004**, *77*, 749–756. [CrossRef]
7. Asaduzzaman, M.; Hasan, M.; Bahar, A.N. An investigation into the effects of band gap and doping concentration on Cu (In, Ga) Se_2 solar cell efficiency. *SpringerPlus* **2016**, *5*, 578. [CrossRef]
8. Alonso, M.I.; Wakita, K.; Pascual, J.; Garriga, M.; Yamamoto, N. Optical functions and electronic structure of $CuInSe_2$, $CuGaSe_2$, $CuInS_2$, and $CuGaS_2$. *Phys. Rev. B* **2001**, *63*, 075203. [CrossRef]
9. Gloeckler, M.; Sites, J.R. Band-gap grading in Cu (In, Ga) Se_2 solar cells. *J. Phys. Chem. Solids* **2005**, *66*, 1891–1894. [CrossRef]
10. Rau, U.; Schmidt, M.; Jasenek, A.; Hanna, G.; Schock, H.W. Electrical characterization of Cu (In, Ga) Se_2 thin-film solar cells and the role of defects for the device performance. *Sol. Energy Mater. Sol. Cells* **2001**, *67*, 137–143. [CrossRef]
11. Hanna, G.; Jasenek, A.; Rau, U.; Schock, H.W. Influence of the Ga-content on the bulk defect densities of Cu (In, Ga) Se_2. *Thin Solid Films* **2001**, *387*, 71–73. [CrossRef]
12. Pettersson, J.; Törndahl, T.; Platzer-Björkman, C.; Hultqvist, A.; Edoff, M. The Influence of Absorber Thickness on Cu (In, Ga) Se_2 Solar Cells with Different Buffer Layers. *IEEE J. Photovolt.* **2013**, *3*, 1376–1382. [CrossRef]
13. Asma, C.; Boumdienne, B.; Meriem, C. Numerical analysis of the effect graded Zn (O, S) on the performance of the graded CIGS based solar cells by SCAPS-1D. *Int. J. Nanoelectron Mater.* **2016**, *9*, 103–110.
14. Movla, H.; Abdi, E.; Salami, D. Simulation analysis of the CIGS based thin film solar cells. *Optik* **2013**, *124*, 5871–5873. [CrossRef]
15. Vermang, B.; Wätjen, J.T.; Fjällström, V.; Rostvall, F.; Edoff, M.; Kotipalli, R.; Henry, F.; Flandre, D. Employing Si solar cell technology to increase efficiency of ultra-thin Cu (In, Ga) Se_2 solar cells. *Prog. Photovolt. Res. Appl.* **2014**, *22*, 1023–1029. [CrossRef]
16. Amin, N.; Chelvanathan, P.; Hossain, M.; Sopian, K. Numerical modelling of ultra thin Cu (In, Ga) Se_2 solar cells. *Energy Procedia* **2012**, *15*, 291–298. [CrossRef]
17. Ahamed, E.I.; Bhowmik, S.; Matin, M.; Amin, N. Highly efficient ultra thin Cu (In, Ga) Se_2 solar cell with tin Selenide BSF. In Proceedings of the 2017 International Conference on Electrical, Computer and Communication Engineering (ECCE), Cox's Bazar, Bangladesh, 16–18 February 2017; pp. 428–432.
18. Song, J.; Li, S.; Huang, C.; Crisalle, O.; Anderson, T.J. Device modeling and simulation of the performance of Cu (In1 − x, Gax) Se_2 solar cells. *Solid-State Electron.* **2004**, *48*, 73–79. [CrossRef]
19. Benabbas, S.; Heriche, H.; Rouabah, Z.; Chelali, N. Enhancing the efficiency of CIGS thin film solar cells by inserting novel back surface field (SnS) layer. In Proceedings of the 2014 North African Workshop on Dielectic Materials for Photovoltaic Systems (NAWDMPV), Tlemcen, Algeria, 26–27 October 2014; pp. 1–5.
20. Omrani, M.K.; Minbashi, M.; Memarian, N.; Kim, D.-H. Improve the performance of CZTSSe solar cells by applying a SnS BSF layer. *Solid-State Electron.* **2018**, *141*, 50–57. [CrossRef]
21. Burgelman, M.; Marlein, J. Analysis of graded band gap solar cells with SCAPS. In Proceedings of the 23rd European Photovoltaic Solar Energy Conference, Valencia, Spain, 1–5 September 2008; pp. 2151–2155.
22. Decock, K.; Khelifi, S.; Burgelman, M. Modelling multivalent defects in thin film solar cells. *Thin Solid Films* **2011**, *519*, 7481–7484. [CrossRef]
23. Göde, F.; Gümüş, C.; Zor, M. Investigations on the physical properties of the polycrystalline ZnS thin films deposited by the chemical bath deposition method. *J. Cryst. Growth* **2007**, *299*, 136–141. [CrossRef]
24. Jackson, P.; Hariskos, D.; Wuerz, R.; Wischmann, W.; Powalla, M. Compositional investigation of potassium doped Cu (In, Ga) Se_2 solar cells with efficiencies up to 20.8%. *Phys. Status Solidi RRL Rapid Res. Lett.* **2014**, *8*, 219–222. [CrossRef]
25. Wei, S.-H.; Zhang, S.; Zunger, A. Effects of Ga addition to $CuInSe_2$ on its electronic, structural, and defect properties. *Appl. Phys. Lett.* **1998**, *72*, 3199–3201. [CrossRef]
26. Khoshsirat, N.; Yunus, N.; Hamidon, M.; Shafie, S.; Amin, N. Analysis of absorber layer properties effect on CIGS solar cell performance using SCAPS. *Optik* **2015**, *126*, 681–686. [CrossRef]
27. Hirai, Y.; Kurokawa, Y.; Yamada, A. Numerical study of Cu (In, Ga) Se_2 solar cell performance toward 23% conversion efficiency. *Jpn. J. Appl. Phys.* **2013**, *53*, 012301. [CrossRef]
28. Gloeckler, M.; Fahrenbruch, A.; Sites, J.R. Numerical modeling of CIGS and CdTe solar cells: Setting the baseline. In Proceedings of the 3rd World Conference on Photovoltaic Energy Conversion, Osaka, Japan, 11–18 May 2003; Volume 1, pp. 491–494.
29. Levcenko, S.; Gurieva, G.; Friedrich, E.; Trigo, J.; Ramiro, J.; Merino, J.; Arushanov, E.; León, M. Optical constants of CuIn1-xGaxSe_2 films deposited by flash evaporation. *Mold. J. Phys. Sci.* **2010**, *9*, 148–155.
30. Luo, K.; Sun, Y.; Zhou, L.; Wang, F.; Wu, F. Theoretical simulation of performances in CIGS thin-film solar cells with cadmium-free buffer layer. *J. Semicond.* **2017**, *38*, 084006. [CrossRef]
31. Chelvanathan, P.; Hossain, M.; Amin, N. Performance analysis of copper–indium–gallium–diselenide (CIGS) solar cells with various buffer layers by SCAPS. *Curr. Appl. Phys.* **2010**, *10*, S387–S391. [CrossRef]
32. Chadel, A.; Benyoucef, B.; Chadel, M. A comparative study of CIGS solar cells based on Zn (O, S) buffer layers and CIGS solar cells based on CdS buffer layers. *Optoelectron. Adv. Mater.-Rapid Commun.* **2015**, *9*, 653–656.
33. Buffière, M.; Harel, S.; Guillot-Deudon, C.; Arzel, L.; Barreau, N.; Kessler, J. Effect of the chemical composition of co-sputtered Zn (O, S) buffer layers on Cu (In, Ga) Se_2 solar cell performance. *Phys. Status Solidi A* **2015**, *212*, 282–290. [CrossRef]
34. Reddy, V.R.M.; Gedi, S.; Pejjai, B.; Park, C. Perspectives on SnSe-based thin film solar cells: A comprehensive review. *J. Mater. Sci. Mater. Electron.* **2016**, *27*, 5491–5508. [CrossRef]

35. Barrios-Salgado, E.; Nair, M.; Nair, P.K. Chemically deposited SnSe thin films: Thermal stability and solar cell application. *ECS J. Solid State Sci. Technol.* **2014**, *3*, Q169. [CrossRef]
36. Mouhoub, A.; Bouloufa, A.; Djessas, K.; Messous, A. Analytical modeling and optimization of original bifacial solar cells based on Cu (In, Ga) Se2 thin films absorbers. *Superlattices Microstruct.* **2018**, *122*, 434–443. [CrossRef]
37. Yuan, J.; Huang, H.; Deng, X.; Yue, Z.; He, Y.; Zhou, N.; Zhou, L. Photoemission cross section: A critical parameter in the impurity photovoltaic effect. *Chin. Phys. B* **2017**, *26*, 018503. [CrossRef]
38. Gloeckler, M.; Sites, J.R. Potential of submicrometer thickness Cu (In, Ga) Se_2 solar cells. *J. Appl. Phys.* **2005**, *98*, 103703. [CrossRef]
39. Jehl, Z.; Erfurth, F.; Naghavi, N.; Lombez, L.; Gerard, I.; Bouttemy, M.; Lincot, D. Thinning of CIGS solar cells: Part II: Cell characterizations. *Thin Solid Films* **2011**, *519*, 7212–7215. [CrossRef]
40. Lundberg, O.; Edoff, M.; Stolt, L. The effect of Ga-grading in CIGS thin film solar cells. *Thin Solid Films* **2005**, *480*, 520–525. [CrossRef]
41. Hossain, S.; Amin, N.; Razykov, T. Prospects of back contacts with back surface fields in high efficiency Zn x Cd_{1-x} S/CdTe solar cells from numerical modeling. *Chalcogenide Lett.* **2011**, *8*, 3.
42. Khosroabadi, S.; Keshmiri, S.H. Design of a high efficiency ultrathin CdS/CdTe solar cell using back surface field and backside distributed Bragg reflector. *Opt. Express* **2014**, *22*, A921–A929. [CrossRef]
43. Todorov, T.K.; Tang, J.; Bag, S.; Gunawan, O.; Gokmen, T.; Zhu, Y.; Mitzi, D.B. Beyond 11% efficiency: Characteristics of state-of-the-art Cu_2ZnSn (S, $Se)_4$ solar cells. *Adv. Energy Mater.* **2013**, *3*, 34–38. [CrossRef]
44. Green, M.A. Accuracy of analytical expressions for solar cell fill factors. *Sol. Cells* **1982**, *7*, 337–340. [CrossRef]
45. Duchatelet, A.; Letty, E.; Jaime-Ferrer, S.; Grand, P.-P.; Mollica, F.; Naghavi, N. The impact of reducing the thickness of electrodeposited stacked Cu/In/Ga layers on the performance of CIGS solar cells. *Sol. Energy Mater. Sol. Cells* **2017**, *162*, 114–119. [CrossRef]
46. Burgelman, M.; Decock, K.; Khelifi, S.; Abass, A. Advanced electrical simulation of thin film solar cells. *Thin Solid Films* **2013**, *535*, 296–301. [CrossRef]
47. Huo, X.X.; Mo, X.; Chen, G.R. Deposition technologies of Cd-free buffer layers in solar cells made of copper indium gallium diselenide films. *Chin. J. Vac. Sin. Tech.* **2012**, *9*, 834.
48. Eisele, W.; Ennaoui, A.; Schubert-Bischoff, P.; Giersig, M.; Pettenkofer, C.; Krauser, J.; Karg, F. XPS, TEM and NRA investigations of Zn (Se, OH)/Zn $(OH)_2$ films on Cu (In, Ga)(S, $Se)_2$ substrates for highly efficient solar cells. *Sol. Energy Mater. Sol. Cells* **2003**, *75*, 17–26. [CrossRef]
49. Negami, T.; Aoyagi, T.; Satoh, T.; Shimakawa, S.; Hayashi, S.; Haskimoto, Y. Cd free CIGS solar cells fabricated by dry processes. In Proceedings of the Conference Record of the Twenty-Ninth IEEE Photovoltaic Specialists Conference, New Orleans, LA, USA, 19–24 May 2002; pp. 656–659.
50. Ramanathan, K.; Mann, J.; Glynn, S.; Christensen, S.; Pankow, J.; Li, J.; Noufi, R. A comparative study of Zn (O, S) buffer layers and CIGS solar cells fabricated by CBD, ALD, and sputtering. In Proceedings of the 2012 38th IEEE Photovoltaic Specialists Conference, Austin, TX, USA, 3–8 June 2012.
51. Okamoto, A.; Minemoto, T.; Takakura, H. Application of sputtered ZnO1-xSx buffer layers for Cu (In, Ga) Se_2 solar cells. *Jpn. J. Appl. Phys.* **2011**, *50*, 04DP10. [CrossRef]
52. Chadel, M.; Chadel, A.; Bouzaki, M.; Aillerie, M.; Benyoucef, B.; Charles, J.-P. Optimization by simulation of the nature of the buffer, the gap profile of the absorber and the thickness of the various layers in CZTSSe solar cells. *Mater. Res. Express* **2017**, *4*, 115503. [CrossRef]
53. Papadimitriou, D.N. Engineering of Optical and Electrical Properties of Electrodeposited Highly Doped Al: ZnO and In: ZnO for Cost-Effective Photovoltaic Device Technology. *Micromachines* **2022**, *13*, 1966. [CrossRef] [PubMed]
54. Huang, C.-H.; Chuang, W.-J.; Lin, C.-P.; Jan, Y.-L.; Shih, Y.-C. Deposition technologies of high-efficiency CIGS solar cells: Development of two-step and co-evaporation processes. *Crystals* **2018**, *8*, 296. [CrossRef]
55. Minbashi, M.; Omrani, M.; Memarian, N.; Kim, D.-H. Comparison of theoretical and experimental results for band-gap-graded CZTSSe solar cell. *Curr. Appl. Phys.* **2017**, *17*, 1238–1243. [CrossRef]
56. Djoumi, S.; Kail, F.; Cabarrocas, P.; Chahed, L. Tin versus indium catalyst in the growth of silicon nanowires by plasma enhanced chemical vapor deposition on different substrates. *Thin Solid Films* **2022**, *758*, 139447. [CrossRef]
57. Ramanujam, J.; Singh, U.P. Copper indium gallium selenide based solar cells—A review. *Energy Environ. Sci.* **2017**, *10*, 1306–1319. [CrossRef]

Disclaimer/Publisher's Note: The statements, opinions and data contained in all publications are solely those of the individual author(s) and contributor(s) and not of MDPI and/or the editor(s). MDPI and/or the editor(s) disclaim responsibility for any injury to people or property resulting from any ideas, methods, instructions or products referred to in the content.